Modeling hydrogen storage at room temperature: Adsorbent materials for boosting pressure reduction in compressed H2 tanks

Journal of Energy Storage 90 (2024) 111758

Contents lists available at ScienceDirect

Journal of Energy Storage

journal homepage: www.elsevier.com/locate/est

Research Papers

Modeling hydrogen storage at room temperature: Adsorbent materials for boosting pressure reduction in compressed H_2 tanks

Francesco Demetrio Minuto *, Elena Rozzi, Romano Borchiellini, Andrea Lanzini

Energy Department, Politecnico di Torino, Corso Duca degli Abruzzi 24, 10129 Torino, Italy
Energy Center Lab, Politecnico di Torino. Corso Duca degli Abruzzi 24, 10129 Torino, Italy

ARTICLE INFO

Keywords:
Hydrogen storage
Adsorbent materials
Tank pressure
Storage efficiency
Power energy services

ABSTRACT

Energy storage systems are required for an efficient integration of renewables into the grid to achieve a net zero energy system. Hydrogen compressed at 700 bar, is one of the key energy storage technologies. This study evaluates the effectiveness of solid-state hydrogen storage, particularly physisorption in porous materials, to enhance storage performance and safety at room temperature by reducing the operating tank pressure. We model dynamically the entire storage system, comparing adsorbent materials to traditional compression in terms of maximum tank pressure and round-trip storage efficiency. Different energy system applications with varied cycle frequencies and discharge durations were examined. Results indicate that porous material-based systems exhibit higher efficiency for long-duration energy storage services than the compressed hydrogen. Notably, bulk density plays a pivotal role in storage performance. For instance, IRMOF-1 with a bulk density of 500 kg/m^3, shows a 70 % pressure reduction compared to compressed hydrogen systems. In contrast, when its bulk density is reduced to 130 kg/m^3, the maximum tank pressure is even 30 % higher than the compressed tank. We emphasize the need for comprehensive material characterization, highlighting the significance of parameters like bulk density for determining the most performing hydrogen adsorbent material in terms of maximum tank pressure and efficiency. As general outcome, the best performing material depends on the specific target or system requirements, such as pressure, volume, cost, or weight.

1. Introduction

In recent years, a growing number of nations have pledged to attain net-zero emissions. As of October 2023, the Net Zero Tracker [1] indicates that 151 countries, accounting for over 90 % of global greenhouse gas emissions, have declared net-zero targets. The IRENA reports that in 2022 [2], new renewables constituted 88 % of the annual power capacity expansion, marking a consistent upward trajectory since 2002. Given the inherently intermittent nature of renewable energy and its significant spatial distribution on the power grid, it's crucial to develop a resilient energy system, capable of transporting and balancing energy between areas of high supply and high demand [3]. Storage systems therefore become crucial for the increase in penetration and integration of renewables, mitigating energy security issue [4].

Among various storage options - including batteries, thermochemical, thermal, pumped energy storage, compressed air, hydrogen, and chemical storage - each providing unique features, advantages, and limitations [5], hydrogen emerge as viable green storage technology, given its capability to store energy generated directly from renewable sources [6], which might play a pivotal role in climate change mitigation [7]. Numerous studies conducted by the European Commission and the US Department of Energy (DOE) have identified hydrogen as a viable alternative energy vector, capable of contributing to meeting long-term energy demands in a variety of sectors including transportation, manufacturing, and residential [8].

The hydrogen economy is challenged by safety concerns, affordability issues, technical limitations, and the absence of standardized regulations, which hinder its broader adoption. Hydrogen storage technologies are primarily divided into physical-based and material-based methods [9]. Physical storage include compressed-H_2, liquid-H_2, and cryo-compressed H_2, where hydrogen is stored or released through pressure adjustments, temperature changes, or both. Material-based

Abbreviations: MOF, Metal-Organic Frameworks; IRENA, International Renewable Energy Agency; LCOS, Levelized Cost Of Storage; NIST, National Institute of Standards and Technology.

* Corresponding author at: Energy Department, Politecnico di Torino, Corso Duca degli Abruzzi 24, 10129 Torino, Italy.
E-mail address: francesco.minuto@polito.it (F.D. Minuto).

https://doi.org/10.1016/j.est.2024.111758
Received 22 December 2023; Received in revised form 25 March 2024; Accepted 17 April 2024
Available online 4 May 2024

storage, referred also as solid-state storage, involve adsorption of hydrogen by physisorption phenomena on porous materials like activated carbon, MOFs, COFs [10], herein called adsorbent materials, or absorption on metal hydrides to store hydrogen by chemisorption phenomena [11,12].

Currently, high-pressure compression is the preferred method for hydrogen storage due to its technological readiness and maturity [13]. Compressed-H_2 is typically stored in vessels designed to withstand pressures up to 700 bar (Type III, metal-lined tanks with full composite wrap). However, these high-pressure vessels face challenges and limitations, such as hydrogen embrittlement in steels, blistering in polymer liners, and damage mechanisms in carbon fiber composite vessels, all dependent on the materials and construction process and materials [15]. Leaked hydrogen, when mixes with air, can create explosive gas clouds, a risk underscored by past pressure vessel incidents [13]. Moreover, hydrogen's tendency to degrade materials that can lead to leaks poses serious hazards issues [14].

One critical approach to enhancing the safety of hydrogen storage is the reduction of tank pressure. The utilization of solid adsorbents has emerged as a promising solution [16] to reduce hydrogen tank pressure. Research into hydrogen adsorption on solid materials is gaining attention because these adsorbents have a high surface area and pore volume, which could significantly increase energy density [17]. However, physisorption is characterized by low enthalpy interactions, making this storage technique more effective at cryogenic temperatures [18]. Consequently, adsorption capacity is often characterize in the literature thorough adsorption isotherm measurements at 77 K, with gravimetric capacity (either excess or absolute) typically reported at the maximum apparatus pressure [21], often below 50 bar. There's been a focus on developing new materials with higher adsorption capacities, including new classes of Metal-Organic Frameworks (MOFs), which have shown considerable potential in experimental and theoretical studies [19]. For example, MOF NU-100 has demonstrated an exceptional hydrogen storage gravimetric capacity of over 10 wt% at 77 K [20]. However, from an application standpoint, the volumetric capacity is more significant than the gravimetric capacity, though less frequently reported in the literature. Over time, to assess the applicability of materials, other metrics such as "net adsorption" and "useful capacity" have been proposed [18]. Despite these efforts, such metrics fall short in providing a comprehensive insight of the materials performance at temperatures higher from 77 K, like ambient temperature, because of the non-linearity of the adsorption isotherms with the temperature.

In terms of energy storage services, hydrogen storage can cover a broad spectrum of time-scale requirements [22]. In energy system applications, it can manage short-term needs like system frequency control, and it is equally adapted for balancing long-term (or seasonal) energy supply and demand. Schmidt et al. [23] provided a comprehensive assessment of the levelized cost of storage (LCOS) for nine electricity storage technologies and twelve power system applications (Table 1). This study concluded that lithium-ion is the most cost-efficient for most applications, especially those requiring less than 4 h of discharge and fewer than 300 annual cycles. While, for seasonal storage needs that surpass 700 h of discharge, hydrogen storage (compressed-H_2) emerges as a the most economical choice.

Table 1
Power system: list and characteristics of energy services.

Energy service	Annual cycles [#]	Discharge duration [hours/cycle]
1. Energy arbitrage	300	4
2. Primary response	5000	0.50
3. Secondary response	995	1
4. Tertiary response	10	4
5. Peaker replacement	50	4
6. Black start	10	1
7. Seasonal storage	3	700
8. Renewable integration	300	8
9. Congestion management	300	1
10. Bill management	500	4
11. Power quality	100	0.5
12. Power reliability	50	8

In this regard, a limited number of authors have explored the performance of adsorbent-based hydrogen storage systems, and exclusively for specific energy applications. Zini et al. [24,25] modeled the use of activated carbon based hydrogen storage, operated at liquid nitrogen temperatures, demonstrating its feasibility for renewable energy-powered residential applications, such as wind and photovoltaic systems. Rozzi et al. [26] examined the advantages of incorporating adsorbent materials in hydrogen storage tanks at room temperature for stationary applications, such as photovoltaic self-consumption enhancement in energy communities. Anastasopoulou et al. [27] conducted a techno-economic analysis, highlighting the potential of MOF-based hydrogen storage for onboard transportation applications. Peng et al. [28] performed a techno-economic analysis of stationary MOF hydrogen storage for backup applications.

However, these studies often focus on narrow applications domains, leaving the broader potential and implications of adsorbent-based hydrogen storage systems across different energy services underexplored. This study aims to address this gap by presenting a systematically investigation into the performance of adsorbent-based hydrogen storage systems across a broad spectrum of power energy services, from renewable integration to seasonal energy storage. By dynamically model the entire storage system and simulating its performance for each energy service individually, this research offers a comprehensive analysis of the applicability of adsorbent materials in hydrogen storage across the entire spectrum of power energy services depicted in Fig. 1.

The novelty of this analysis lies in the assessment of the effectiveness of adsorbent-based hydrogen storage system, operating at room temperature, across various power energy services. Our contribution is twofold. Firstly, we elucidate the influence of material properties, particularly bulk density, on system performances (operating pressure and roundtrip efficiency). Secondly, we offer a methodology and demonstrate how to identify the most suitable adsorbent materials across diverse energy services.

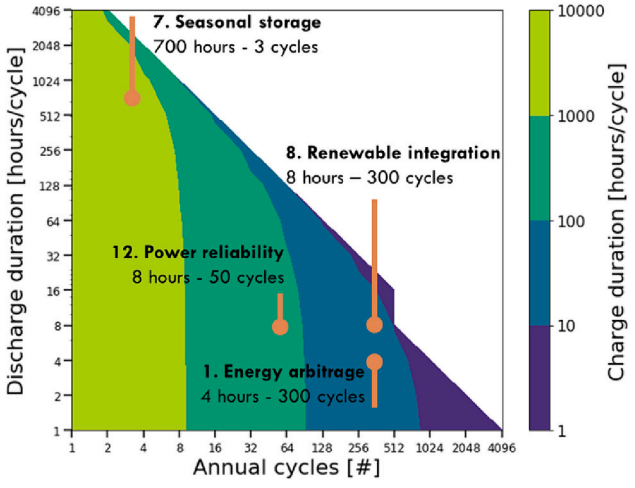

Fig. 1. Power energy services domain explored through simulations. This figure illustrates the domain of energy services investigated, with discharge duration on the y-axis and annual cycles on the x-axis. Charge duration is denoted by the color scale. The oblique boundary delineates the condition where charge and discharge durations are equal. Some of the energy services in Table 1 are mapped within this domain (such as energy arbitrage, seasonal storage, renewable integration, and power reliability).

2. Materials and methods

In our research, we aim to comprehensively test the performance of the hydrogen storage system under various energy storage services conditions. To achieve this goal, we have constructed a two-level simulation environment. The first level systematically simulates the storage response to different energy services by parametrically generating a charge/discharge profile for each point within the domain of energy services (described in Section 2.1). The second level simulates the dynamic behavior of a power-to-power storage system at room temperature within an operational pressure range up to 700 bar, given a timeseries of charge/discharge for the storage (described in Section 2.2).

2.1. Energy services scenario and simulation framework

The methodology adopted simulates the storage system's behavior across different discharge durations and annual cycle counts by synthetically generating energy demand and production profiles, investigating its efficiency and capabilities.

We model the single power energy service as a charge-discharge event having a specific duration and frequency over the year. To analyze the diversity of such services, we examine different combinations characterized by their frequency, i.e., the number of cycles per year, and their discharge duration. Given that there are 8760 h in a year, the duration of the charging period (t_c) for each cycle is determined by the following equation:

$$t_c = \frac{8760}{frequency} - t_d \tag{1}$$

where t_d represents the discharge duration, and frequency denotes the number of annual cycles.

This model allows us to explore the operational dynamics of energy storage systems under different conditions of use. The investigated power energy service domain is illustrated in Fig. 1.

The tank volume of 12.5 m^3 is sized to store a maximum capacity of 10 MWh of compressed hydrogen at 300 bar. Demand and energy surplus profiles are parametrically generated using a synthetic load algorithm. The algorithm output is a net load profile, derived from subtracting the load demand profile from the generation profile, which represents the power flow experienced by the storage system (see Fig. 2-left). The positive values of the net load profile represent excess energy fed into the storage, while negative values indicate energy demand requested from the storage. In each simulation, the excess energy per cycle is set at 10 MWh, and the energy demand is set at 4 MWh (considering a maximum roundtrip storage efficiency of 0.4). Synthetic net load profile used to generate the power energy service map are reported in the open source database [29], while examples for energy arbitrage (4-h discharge and 300 cycles a year) and renewable integration (8-h discharge, 300 cycles a year) services are depicted in Fig. 2-right.

The fuel cell size is determined to deliver the energy at a constant rate throughout the discharge phase. The charging phase can be of equal duration to the discharge or longer. Then, the electrolyzer is sized to charge at a steady power throughout the whole charging phase.

2.2. Hydrogen storage simulation

The hydrogen storage system is an extension of our previous work [26]. The storage system comprises the following zero-dimensional components: the electrolyzer, a multi-stage compressor, the hydrogen tank, and the fuel cell (see Fig. 3). The tank can either be empty or filled with adsorbent materials. Each component is dynamically simulated. The main characteristics of the modeled devices are summarized in Appendix A. For a comprehensive description of the storage system, its components' equation, and validation, readers are referred to [26].

The storage is initialized under vacuum. During the charge phase, hydrogen supplied by the electrolyzer is compressed and filled into the tank. The electrolyzer, compressor, and fuel cell are equipped with a temperature management system to keep the components temperature within their operating range. Besides, the hydrogen injected into the storage is cooled before being introduced into the tank. The tank is assumed to be in thermal equilibrium with its surroundings, thus maintaining a storage temperature of 298 K. During the discharge phase, hydrogen is released from the tank to feed fuel cell stack at 2 bar.

The Proton Exchange Membrane (PEM) electrolyzer model includes anode and cathode electrodes, a Nafion-117 electrolyte membrane, a gas diffusion layer, and an interconnector plate. The model employs principles of mass balance, charge transport, and electrochemical kinetics. When operating above the thermoneutral voltage, it generates heat, necessitating cooling. The stack temperature is calculated using a simplified, quasi-steady-state thermal method. The hydrogen outlet pressure is set at 30 bar.

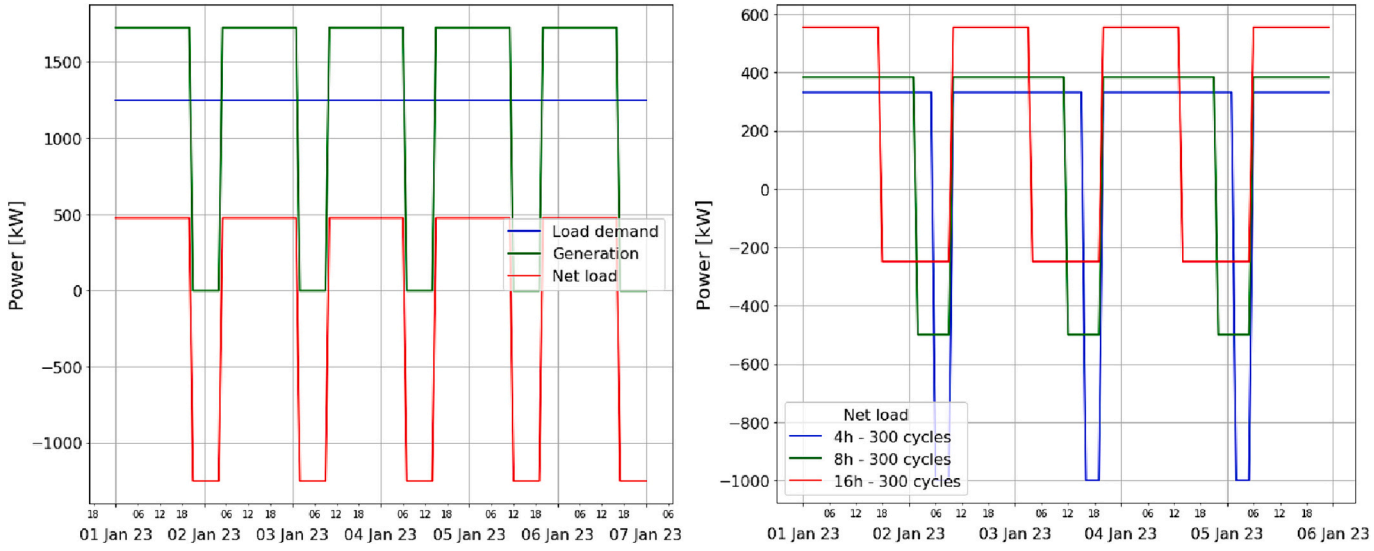

Fig. 2. Illustration example of the outputs from the synthetic load algorithm. Left: The net load profile, derived from subtracting the load demand profile from the generation profile; Right: Synthetic net load profiles for three power energy services with identical annual cycle counts. Each profile delivers, during the discharge phase (negative power), the same amount of energy but at different rates.

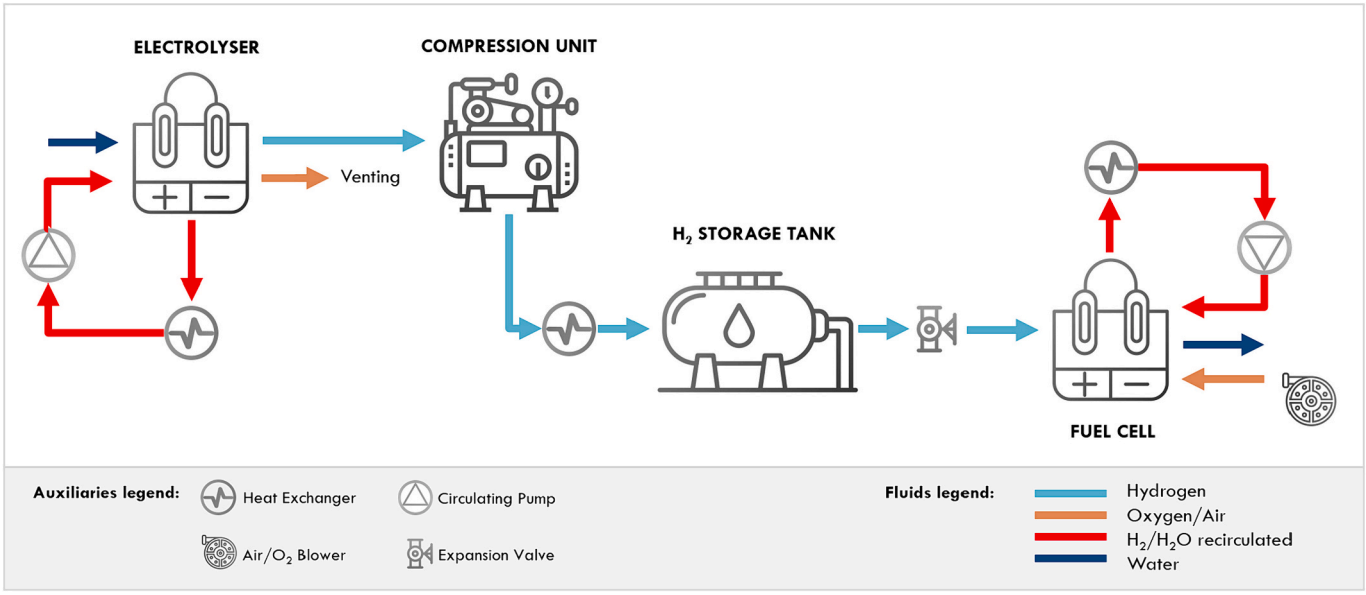

Fig. 3. Representation of the hydrogen storage system simulation framework.

The compression model elaborates the hydrogen coming from the electrolyzer. We represent the compressor as a multi-stage diaphragm compressor with interstage gas cooling. Hydrogen is compressed and cooled from its initial state at the electrolyzer's outlet to the desired tank pressure and ambient temperature. The compressor's outlet pressure maintains an overpressure of 5 bar compared to the storage tank's internal pressure. The model determines the number of stages, ensuring each stage's compression ratio doesn't surpass 6 and the temperature stays below 423 K. Key parameters like compression ratio, isentropic efficiency, and mechanical efficiency are incorporated.

The tank pressure is modeled calculating the amount of hydrogen introduced into the storage by the compressor, or delivered to the fuel cell, and deriving it from the hydrogen volumetric total capacity isotherm at room temperature for the case of empty tank (compressed-H_2) or filled with porous materials (adsorbed in the porous material). The volumetric total isotherm for an empty tank is sourced from the NIST database on thermochemical fluids, while adsorption materials have been selected from the NIST adsorbent database [30]. Due to scarcity of experimental data of adsorption capacity and bulk density, we selected three adsorbents - IRMOF-1 [31], C/Be_2 [32], and NU-110 [33] - for which experimental data where available within our operation range (up to 700 bar and room temperature). In Fig. 4, are reported the gravimetric total hydrogen adsorption isotherms for the IRMOF-1, C/Be_2, and NU-110 adsorbents determined by fitting experimental data, using the Dubinin-Astakhov equation [30]. The adsorption/desorption isotherms coincide as for these materials physisorption is fully reversible. Given the storage tank volume and the amount of storage material packed in the tank, the adsorbents volumetric isotherm is derived using the bulk density reported in the literature, and summarized in Table 2.

As for the electrolysis stack, the fuel cell electrochemical model integrates mass balance, charge transport, and electrochemical kinetics. The polarization curve is assessed across a temperature range (298–353 K), capturing dynamic operation during cold start-ups. Both anode and cathode operating temperatures setpoint is 353 K. A circulating water extract the generated heat which released in the ambient thorough the heat exchanger.

The simulation input is the net load profile, which is the difference between electricity generation and demand, where positive values represent energy supplied to the electrolyzer, while negative values indicate electricity requested to the fuel cell. The simulation output used

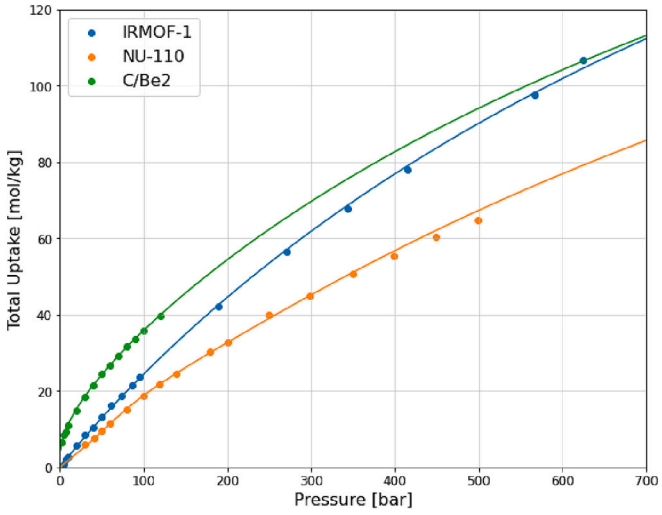

Fig. 4. Total hydrogen adsorption isotherms at 298 K for the investigated adsorbent materials; dots: experimental data from NIST database; solid line: fit of experimental data using the Dubinin-Astakhov equation.

Table 2
Bulk density values for IRMOF-1, C/Be_2, and NU-110.

	IRMOF-1	C/Be_2	NU-110
Powder bulk density [kg/m^3]	130; Ref. [34]	–	222; Ref. [33]
Optimized bulk density [kg/m^3]	500; Ref. [34]	500; [26]	500; Ref. [34]

to compare the solid-state hydrogen storage with the compressed-H_2 are the storage system efficiency and the tank's maximum pressure achieved during a year of operation. Where the round-trip storage system efficiency is defined as:

$$\eta = \frac{E_{FC}}{E_{EC} + E_{comp} + E_{aux}} \tag{2}$$

where E_{FC} is annual energy delivered by the fuel cell, and E_{EC}, E_{comp}, E_{aux}

are the electrolyzer, compressor and auxiliary systems (inverters, circulation pumps, blower) energy consumption.

3. Results

This section presents the findings of our analysis. We begin by examining the performance of adsorbent materials in comparison to compressed-H_2 for a specific energy service, i.e. "renewable integration" (8 h – 300 cycles). Then we delve into how structural characteristics of the samples influence the overall outputs. Finally, we provide a comparative analysis between a IRMOF-1 based and a compressed-H_2 storage across the entire operational map of energy services. Last, we extend the comparison among all adsorbent materials to identify the best performing materials across the whole power energy service domain.

Fig. 5-left displays the maximum pressure achieved by the storage system for compressed-H_2 and the three adsorbent materials considered in this study: IRMOF-1 (also known as MOF-5), C/Be_2, and NU-110. A tank filled solely with compressed hydrogen reaches a pressure of approximately 200 bar to store 10 MWh of energy in a 12.5 m^3 volume at ambient temperature. It is evident that configurations with adsorbent-filled tanks significantly reduce pressure. Specifically, there's a pressure reduction of −60 % (75 bar) for NU-110, −70 % (55 bar) for IRMOF-1, and − 80 % (40 bar) for C/Be_2.

This pressure behavior directly influences system efficiency (Fig. 5-right). As pressure decreases, the efficiency proportionally increases. Compared to the 32 % efficiency achieved by compressed-H_2, there's a 3 % efficiency increase due to the reduced pressure from the adsorbent materials.

Among the adsorbent materials measured IRMOF-1 exhibits promising performance, surpassed only by the theoretical performance of the C/Be_2 material, which has not yet been synthesized and experimentally characterized. Besides, it's worth investigating how the structural characteristics of materials, especially the bulk density, impact the simulation outputs. Bulk density, also known as apparent density or pack density, represents the physical volume occupied by the material. Given the known volume of the tank, it determines the amount of adsorbent material that can be contained within the storage. Table 3 presents two distinct bulk density values for IRMOF-1 reported in literature. An intermediate value of 350 kg/m^3 is introduced for sensitivity analysis.

Fig. 6-left compares the maximum pressure between compressed gas and IRMOF-1 across the three considered bulk densities. The previously observed −70 % pressure reduction for IRMOF-1 with a bulk density of 500 kg/m^3 decreases to −56 % for a density of 350 kg/m^3 (labeled as IRMOF-1 (b)). Intriguingly, for an apparent density of 130 kg/m^3 the maximum pressure surpasses that of compressed-H_2 (+30 %), reaching 260 bar. As depicted in Fig. 6-right, when using the efficiency of compressed-H_2 as a reference, pressure increases efficiency in the cases of IRMOF-1 (a) and (b). However, efficiency decreases for IRMOF-1(c).

Table 3
Bulk density values of IRMOF-1 utilized in the sensitivity analysis.

	IRMOF-1 (a)	IRMOF-1 (b)	IRMOF-1 ©
Bulk density [kg/m^3]	500 [34]	350	130 [34]

To get a broader perspective on these results, we present a side-by-side comparison of the maximum pressure achieved by the tank with compressed-H_2 (Fig. 7-left) and IRMOF-1 (a) (Fig. 7-right) across the entire operational map of energy storage services. The color map scale indicates the pressure, the yellow color refers to the highest value obtained in the respective configurations. Specifically, yellow represents a pressure of 213 bar for the compressed tank and 64.5 bar for IRMOF-1 filled tank. For compressed-H_2, the peak of the color scale is at 213 bar, corresponding to a 2-h service cycled 2048 times annually. The lowest pressure, 189 bar, is observed for 16-h services with 512 annual cycles. In contrast, IRMOF-1 peaks at 64.5 bar for 2-h services with 2–8 annual cycles. The predominant pressure, represented by the most extensive uniform color area on the map, stands at 200 bar for compressed-H_2 and 60 bar for IRMOF-1. The maximum pressure across the whole energy service map fluctuates by 11 % for compressed-H_2 and 15 % for IRMOF-1. Interestingly, the pressure disparity between the two tank configurations at parity of operational conditions remains relatively stable, with a consistent difference of approximately −70.6 ± 0.8 %.

Upon examining both maps, we understand that for a given discharge duration, the maximum pressure often remains independent of the number of annual cycles. However, for discharge durations less than a day, a lower number of cycles corresponds to a higher maximum pressure requirement.

Fig. 8 compares the overall efficiency of the storage system between the two configurations. Here, the color scale is normalized to 42 % for both maps, offering a direct comparison.

The efficiency appears constant in values based on discharge duration. The highest efficiency values, up to 40 %, are achieved for longer discharge durations typically seen in the long-term energy storage services sector. Conversely, shorter discharge durations result in reduced

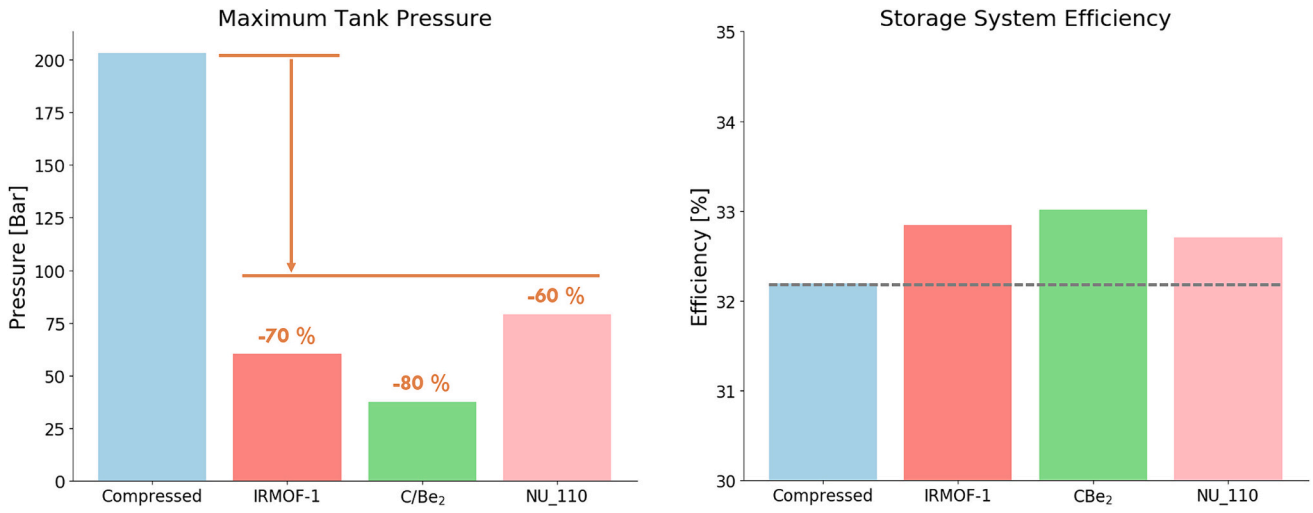

Fig. 5. Comparison of storage performance for renewable integration energy service (8 h – 300 cycles) with different tank fillings: Compressed-H_2 (empty tank), IRMOF-1, C/Be_2, and NU-110. Left: Maximum tank pressure. Right: Storage system efficiency.

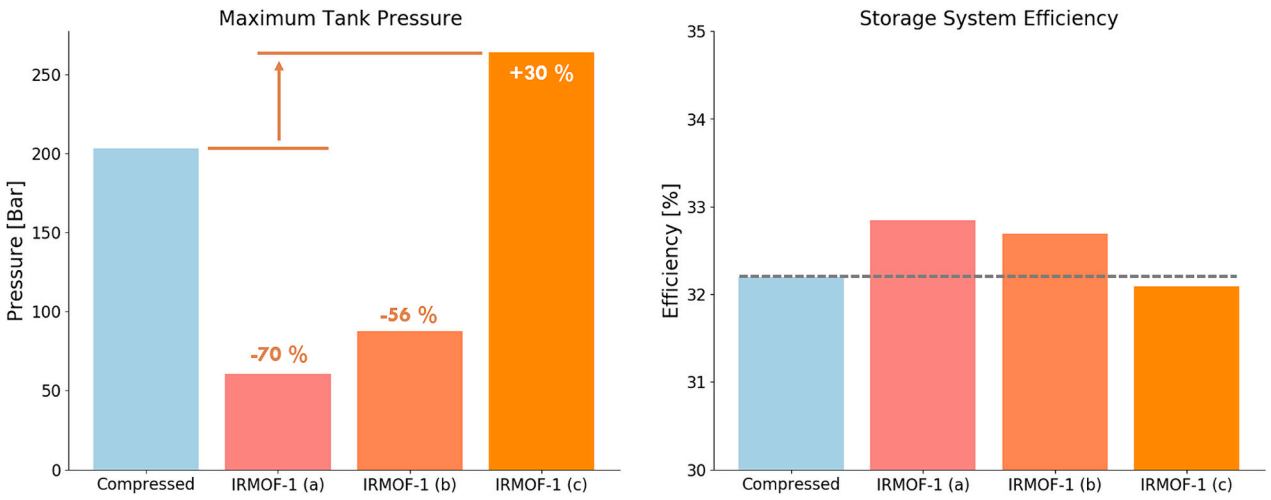

Fig. 6. Comparison of storage performance for renewable integration energy service (8 h - 300 cycles) with different tank fillings: Compressed-H_2 (empty tank) and IRMOF-1 at varying bulk densities. Left: Maximum tank pressure. Right: Storage system efficiency.

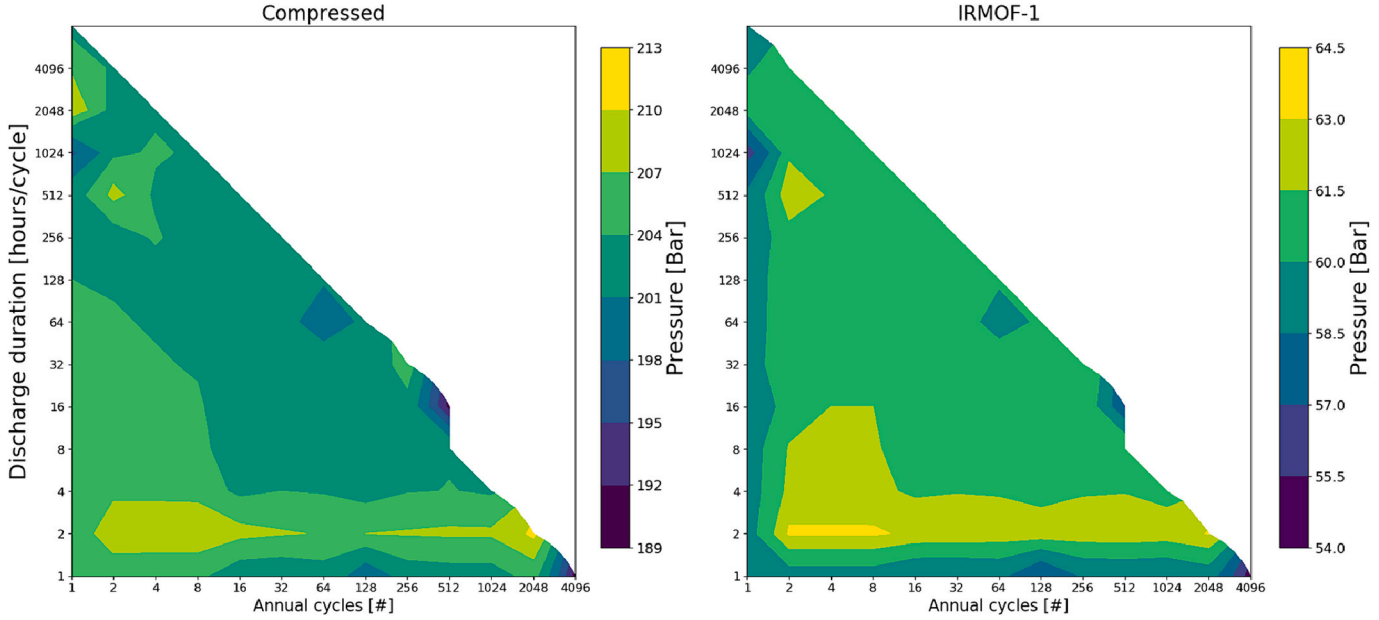

Fig. 7. Maximum tank pressure across the entire power energy service domain. Left: Compressed-H_2 (empty tank). Right: IRMOF-1 filled tank.

efficiency, with a minimum of 18 % for durations less than 2 h and 1 cycle per year.

While the efficiency for compressed-H_2 and IRMOF-1 appear similar in terms of average values and distribution across the map, a closer examination reveals a distinct advantage for IRMOF-1. Specifically, the IRMOF-1 tank showcases a broader operational region with superior efficiency compared to compressed-H_2 tank. This region is highlighted by the dashed black triangle in Fig. 8.

In Fig. 9, we introduce a representation of the power energy service domain, where each point of the map indicates the best performing material among the three investigated in this study, in comparison to compressed-H_2. Fig. 9-left focuses on identifying the best-performing material based on round-trip storage efficiency, while Fig. 9-right emphasizes the optimal material in terms of pressure. The color indicates the percentage variation compared to the compressed hydrogen tank.

Upon examining efficiency (Fig. 9-left), it's evident that no single material consistently outperforms compressed-H_2 across the entire operational area. However, specific zones emerge where certain materials have a clear advantage. For instance, in the region of long-duration energy storage services, IRMOF-1 tends to be superior. In other regions, C/Be_2 often emerges as the top performer. NU-110 only takes the lead in select areas of the map. The color scale reveals that the efficiency improvement over compressed gas typically ranges between 1 % and 5 %, with peaks reaching up to 12 %.

Turning to the pressure map (Fig. 9-right), C/Be_2 stands out as the dominant material across the entire operational spectrum. The pressure difference between C/Be_2 and compressed-H_2 spans between 155 and 185 bar.

4. Discussion

In this study, we systematically analyzed the performance of a 12.5 m^3 hydrogen-based storage system operating at ambient temperature and fed with 10 MWh/cycle of surplus generated energy. By varying discharge length and annual cycles, we investigated various operational conditions corresponding to specific energy services that a storage

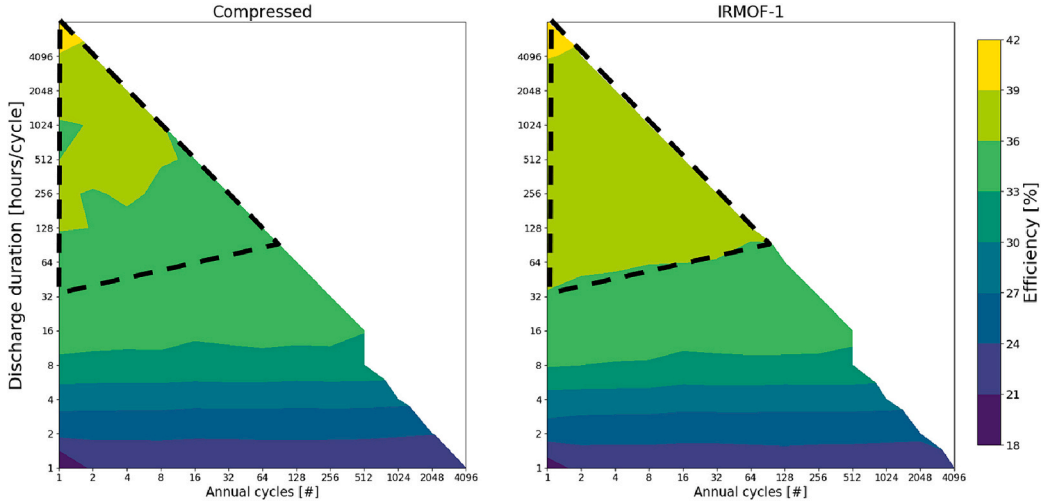

Fig. 8. Efficiency of the storage system across the entire power energy service map. Left: Compressed-H_2 (empty tank). Right: IRMOF-1 filled tank. The black dashed triangle is added as guide for the eye.

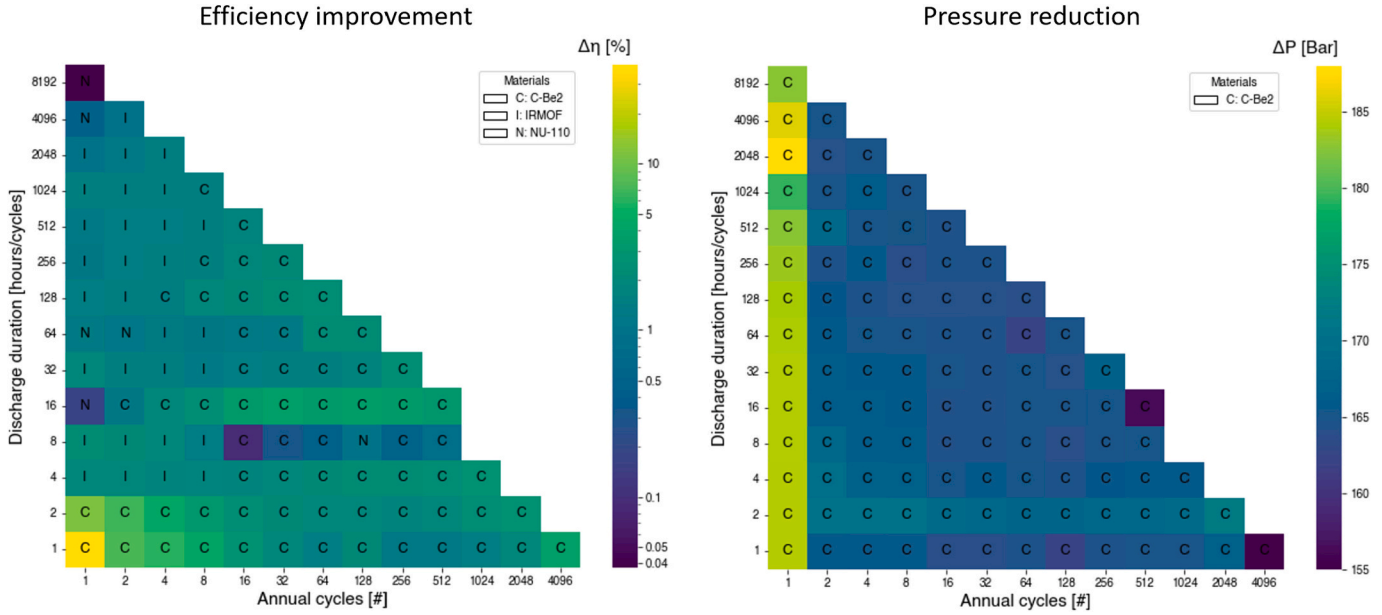

Fig. 9. Best performing material for efficiency and pressure across the entire power energy service map. Left: Efficiency improvement with top performing adsorbent over compressed-H_2 (empty tank). Right: Optimal material by pressure reduction. Adsorbents legend: 'I' for IRMOF-1, 'C' for C/Be, 'N' for NU-110.

system might offer to the grid. The primary objective is to investigate whether incorporating adsorbent materials within the tank could enhance the storage system's performance in terms of maximum required pressure and overall round-trip efficiency, with respect to traditional compressed hydrogen storage. Our analysis did not aim to exhaustively examine a broad range of adsorbents to identify the best materials for various power applications. Instead, it focused on demonstrating a methodological approach by using three materials, found in the literature, with well-documented adsorbent properties within the operational range.

To contextualize our findings, it's important to note that while ambient temperature hydrogen storage is a key goal for many applications [35], the literature often associates hydrogen adsorption on adsorbent materials with cryogenic conditions, where adsorbent materials exhibit their highest adsorption capacities. At higher temperatures, such as at room temperature, achieving the maximum adsorption capacity necessitates very high pressures. This leads to a storage capacity often ranging between 0.5 and 1 wt%, at moderate pressure, which is generally considered insufficient for hydrogen storage applications. For these reasons, most research on adsorbent-based hydrogen storage has focused on cryogenic temperatures rather than room temperature.

Contrary to this conventional viewpoint, our research presents a scenario in which adsorbent materials, operated at ambient temperature, are capable to enhance the performances of compressed hydrogen storage, as illustrated in Fig. 5 and Fig. 7. Specifically, the three adsorbent materials are evaluated in our study—IRMOF-1, NU-110, and C/Be_2 — with their adsorption capacities at room temperature reported as 1.1 wt%, 0.9 wt%, and 2.8 wt% respectively at 20 bar. These materials significantly reduce tank pressure by more than 50 %, and system's efficiency increase of about +3 %. However, it's important to note that these promising results are highly dependent on the bulk density of the materials (Fig. 6). As bulk density decreases, the amount of material that can be physically inserted into the tank reduces, impacting the total physisorbed hydrogen and the gaseous hydrogen volume in the tank.

While, the efficiency gains are primarily attributed to the reduced need for compression to achieve high pressure.

By expanding our analysis across the entire power energy services domain (illustrated in Fig. 8) - namely, by varying the storage charge and discharge duration and number of cycle per year - we observed a reduction in system efficiency for application with shorter discharge durations. This decrease can be due to the suboptimal performance of both the electrolyzer and fuel cell, primarily caused by cold-start losses. Indeed, the frequent cycles of start-up and shutdown, combined with short operational time, prevent the electrochemical devices from reaching and maintaining their optimal operational temperature of 353 K, resulting in an efficiency decline. As a general outcome, we can highlight that the enhancement of energy efficiency through adsorption phenomenal appears limited and more pronounced within the domain of long-term energy service. These findings confirm that hydrogen storage is suitable for long-duration or seasonal storage and less so for intermittent renewable integration into the grid.

The main results highlighted in Fig. 9 indicate that adsorbent materials outperform the compressed hydrogen in terms of both operating pressure and system efficiency across all investigated energy services.

Our findings are consistent with those in the literature that concentrate on a single energy service, yet we offer a comprehensive overview across all energy services. In particular, Zini et al. [24] model a hydrogen storage using adsorbent materials for residential use, powered by a photovoltaic system, using AX-21 activated carbon with a bulk density of 300 kg/m^3 as the adsorbent. Their system, operating through swing adsorption between 77 K and 153 K, achieves about 3 cycles annually with a discharge lasting over 500 h, thus serving as seasonal storage. They reported a storage efficiency of 36 %, similar to our results presented in Fig. 8 for a 500-h discharge at 3 cycles per year. However, when accounting for the energy needed for thermal management at cryogenic temperature, this efficiency drops to 9.5 %. In another study, Zini and Tartarini [25] evaluate the performance of a self-sufficient microgrid (with a 6.4 MWh/year load demand) powered by wind energy and balanced by an adsorbent-based hydrogen storage system. Given the variability of the wind resource, the storage system undergoes about 8 cycles per year with discharges of approximately 500 h, categorizing the storage service within the domain of "Renewable integration" (see Table 1). The storage is filled with AX-21 and it is operated in a swing mode, being charged up to 60 bar at 77 K and discharged by increasing the temperature to 153 K. Similar to the previous work, the overall system efficiency is 13.5 %, primarily due to the thermal management of storage at cryogenic temperatures.

In a previous work [26], we explored the use of an adsorption-based hydrogen storage system as seasonal storage (1 cycle per year with 4300 discharge hours) for an energy community of 100 members (with a 200 MWh/year load demand), powered by a photovoltaic system generating 350 MWh/year. The storage is operated at room temperature and pressures up to 350 bar, with volumes ranging from 50 m^3 to 300 m^3. Depending on the operating conditions, such as adsorbent material, pressure, and tank volume, the energy storage capacity varied from 35 MWh to 47 MWh, while round-trip storage efficiency ranged from 39 % to 43.5 %. These results are consistent with the outcomes of this work in terms of storage efficiency for long term storage service (reported in Fig. 8).

This work addresses a gap left by previous studies, which did not systematically evaluate performance across various energy services or compare the pressure reduction advantages of using adsorbents with those of compressed hydrogen storage for an equivalent amount of stored energy.

Another contribution of this study is the methodology for selecting the most suitable adsorbent material across the diverse energy services. In our analysis appears that while some materials excel in certain conditions, no single material consistently outperforms others across all operational scenarios. Furthermore, considering that adsorbent materials may increase the cost or weight of the storage system, selecting the best material for a particular application should also take into account specific system requirements, such as tank pressure, system volume, additional costs, round-trip system efficiency, and added weight.

Acknowledging the limitations of this study, the accuracy of our findings is dependent on the specified boundary conditions and the accuracy of the input data, for example adsorption isotherm and bulk density data. Therefore, our results should not be viewed as definitive. Despite these limitations, the essential contribution of our research is to show how storage performance differs across various energy services and to illustrate the unique responses of materials under different conditions.

One limitation of our study is the use of constant generation/demand profiles during charge or discharge periods. This has implications for the optimal sizing of the electrolyzer and fuel cell, which then operate at nominal power without transients. These conditions yield the highest obtainable efficiencies, which would be lower under intermittent energy conditions.

Another factor, as reported in literature but not considered in our results, is the significant measurement error on adsorption isotherms at ambient temperatures, especially for pressures above 100 bar. Besides, our adsorption model does not account for the kinetics of adsorption/desorption or potential variations in these kinetics with changes in the bulk density of the materials. It is worth noting that experimental data at room temperature are scarce, for example, bulk density or adsorption/desorption kinetic measurements are not consistently documented in the literature. As final remarks, we want to clarify that our benchmark is limited to only three adsorbent materials, mainly to illustrate the proposed methodology. A more exhaustive benchmarking analysis would ideally utilize extensive adsorption databases featuring hundreds of different adsorbent materials.

5. Conclusions

This research evaluates the effectiveness of adsorbent materials in lowering the operating pressure of stationary hydrogen storage system at room temperature for various power services applications, from arbitrage to long-term storage. To test out hypotheses we use in our simulations three adsorbent materials whose adsorption properties were reported in the literature at room temperature up to high pressures. Compressed hydrogen storage served as the benchmark for our comparison. This investigation has reported the following evidence:

- The use of adsorbent materials in hydrogen storage tanks at room temperature can lead to a significant reduction of operational pressure, i.e. up to −70 % for a IRMOF-1 with a 500 kg/m^3 bulk density. Such reductions might improve safety, longevity, and costs associated with hydrogen storage.
- The bulk density of the adsorbent materials play a critical role on storage system's performance, i.e. for the same energy service an IRMOF-1 with a 130 kg/m^3 bulk density would increase the operating pressure up to +30 % with respect to the compressed configuration. Therefore, bulk density is identified as a key parameter, equally important as the material's adsorption capacity, in the selection of materials for hydrogen storage applications.
- We demonstrate, using three adsorbent materials as an example, that selecting the best material depends on the specific operational conditions and requirements of the system, such as roundtrip efficiency, operational pressure, and other, like to system weight, or costs.
- The study reaffirms the viability of hydrogen storage for long-duration or seasonal storage where the roundtrip efficiency exhibited its maximum around 40–42 %. In other energy applications, like in the domain of "renewable energy integration" applications the usage of suitable adsorbents materials can improvement the roundtrip efficiency up to +3 % (i.e. 35 % efficiency) with respect to compressed hydrogen storage (32 %).

The insights derived from this research can inform future adsorbent material development and optimization, guiding the path towards enhanced hydrogen-based energy storage solutions. In our perspective, future research should focus on several key aspects:

- Conduct systematic experimental research on materials adsorption performances operating around room temperature and up to 300 bar. This would help in creating a comprehensive database required for simulating adsorbent-based stationary hydrogen storage operating at ambient temperature.
- Ensure that experimental studies on materials' adsorption performance should report systematically the materials' bulk density. This information is crucial to assess the volumetric storage capacity.
- Conduct a systematic exploration of a wide range of adsorbent materials, using the methodology proposed in this work, to sort out the most promising adsorbent material for various energy service applications.
- Investigate experimentally the interplay between electrolyzer and fuel cell efficiencies when adsorbent materials are used, to understand how these elements can be optimized together.
- Reveal the specific mechanisms by which bulk density and diffusion kinetics affect storage performance, to guide material selection and system design for optimal efficiency.

CRediT authorship contribution statement

Francesco Demetrio Minuto: Writing – review & editing, Writing – original draft, Visualization, Methodology, Investigation, Data curation, Conceptualization. **Elena Rozzi:** Writing – review & editing, Visualization, Software, Methodology, Investigation, Data curation. **Romano Borchiellini:** Writing – review & editing, Supervision, Funding acquisition. **Andrea Lanzini:** Writing – review & editing, Supervision, Methodology, Funding acquisition, Conceptualization.

Declaration of competing interest

The authors declare the following financial interests/personal relationships which may be considered as potential competing interests: Francesco Demetrio Minuto reports financial support was provided by FSE REACT-EU - PON Ricerca e Innovazione 2014–2020. Andrea Lanzini reports financial support was provided by Italian Ministry of the Environment and Energy Security. Elena Rozzi reports financial support was provided by Italian Ministry of the Environment and Energy Security. If there are other authors, they declare that they have no known competing financial interests or personal relationships that could have appeared to influence the work reported in this paper.

Data availability

Data will be made available on request.

Acknowledgments

F.D. Minuto carried out this study within the Ministerial Decree no. 1062/2021 and received funding from the FSE REACT-EU - PON Ricerca e Innovazione 2014-2020.

A. Lanzini and E. Rozzi carried out this study within the National Recovery and Resilience Plan (PNRR) and received funding by the Italian Ministry of the Environment and Energy Security, project "Novel Materials for Hydrogen storage (NoMaH)", ID RSH2A_000035, CUP: F27G22000180006.

This manuscript reflects only the authors' views and opinions, neither the European Union nor the European Commission can be considered responsible for them.

Appendix A

Proton exchange membrane electrolyzer	
Feature	• Electrochemical model based on mass balance, mass and charge transport, and electrochemical kinetics. • Polarization curves at temperature between 298 K and 353 K (in step of 1 K) • Stack thermal management
Representative Equation	$V_{cell}(i) = OCV + \eta_{act.an}(i) + \eta_{act.cat}(i) + \eta_{diff.an}(i) + \eta_{diff.cat}(i) + \eta_{ohm}(i)$ [26]
Input/Output	Input: electric power, storage state-of-charge, stack temperature Output: water supplied, hydrogen flow rate, stack efficiency, thermal fluxes, stack temperature
Multi-stage compressor	
Feature	• Mechanical compression with intercooling • Compression ratio not exceed 6 and discharge temperature not exceed 423 K
Representative Equation	$W_{actual} = \frac{n_{H2}}{\eta_m \eta_{is}} \sum_i \frac{k}{k-1} Z_{avg} R T_s \left[\left(\frac{P_d}{P_s} \right)^{\frac{k-1}{k}} - 1 \right]$ [26]
Input/Output	Input: hydrogen flow rate, tank pressure, hydrogen temperature Output: compression power requirement, number of stages, mechanical and thermal losses
Hydrogen storage	
Feature	• Compressed hydrogen storage modeled as a function of stored hydrogen density and temperature • Hydrogen adsorption into solid materials modeled as a function of total adsorption isotherms
Representative Equation	Hydrogen density: $\rho = \frac{p}{Z(p,T)RT} = \frac{p}{1 + \sum_i^9 a_i \left(\frac{100K}{T} \right)^{b_i} \left(\frac{p}{1MPa} \right)^{c_i}}$ [26] Total adsorption isotherm: $n_{tot} = n_{max} exp \left[- \left(\frac{RT}{\alpha + \beta T} \right)^2 ln^2 \left(\frac{P_0}{P} \right) \right] \widetilde{\rho}_{H2} \left(\frac{1}{\rho_{bulk}} - \frac{1}{\rho_{He}} \right)$ [26]
Input/Output	Input: storage state-of-charge, hydrogen flow rate Output: hydrogen pressure into the tank and storage state-of-charge
Proton exchange membrane fuel cell	
Feature	• Electrochemical model based on mass balance, mass and charge transport, and electrochemical kinetics • Polarization curves at temperature between 298 K and 353 K (step of 1 K) • Stack thermal management
Representative Equation	$V_{cell}(i) = OCV - \eta_{act.an}(i) - \eta_{act.cat}(i) - \eta_{diff.an}(i) - \eta_{diff.cat}(i) - \eta_{ohm}(i)$ [26]
Input/Output	Input: electric power, storage state-of-charge, stack temperature Output: air supplied, hydrogen flow rate, stack efficiency, thermal fluxes, stack temperature

References

[1] Net Zero Tracker, Net Zero Tracker. https://zerotracker.net/, 2023. (Accessed 24 October 2023).

[2] Renewable capacity statistics 2023. https://www.irena.org/Publications/2023/Mar/Renewable-capacity-statistics-2023, 2023 (accessed October 24, 2023).

[3] T. Strasser, F. Andrén, J. Kathan, C. Cecati, C. Buccella, P. Siano, P. Leitão, G. Zhabelova, V. Vyatkin, P. Vrba, V. Mařík, A review of architectures and concepts for intelligence in future electric energy systems, IEEE Trans Ind Electron 62 (2015) 2424–2438, https://doi.org/10.1109/TIE.2014.2361486.

[4] H. Kojima, K. Nagasawa, N. Todoroki, Y. Ito, T. Matsui, R. Nakajima, Influence of renewable energy power fluctuations on water electrolysis for green hydrogen production, Int. J. Hydrogen Energy 48 (2023) 4572–4593, https://doi.org/10.1016/j.ijhydene.2022.11.018.

[5] K.M. Tan, T.S. Babu, V.K. Ramachandaramurthy, P. Kasinathan, S.G. Solanki, S. K. Raveendran, Empowering smart grid: a comprehensive review of energy storage technology and application with renewable energy integration, Journal of Energy Storage 39 (2021) 102591, https://doi.org/10.1016/j.est.2021.102591.

[6] B. Pivovar, N. Rustagi, S. Satyapal, Hydrogen at scale (H2@scale): key to a clean, economic, and sustainable energy system, Electrochem. Soc. Interface 27 (2018) 47, https://doi.org/10.1149/2.F04181if.

[7] J.-N. Kang, Y.-M. Wei, L.-C. Liu, R. Han, B.-Y. Yu, J.-W. Wang, Energy systems for climate change mitigation: a systematic review, Appl. Energy 263 (2020) 114602, https://doi.org/10.1016/j.apenergy.2020.114602.

[8] F. Qureshi, M. Yusuf, M. Arham Khan, H. Ibrahim, B.C. Ekeoma, H. Kamyab, M. M. Rahman, A.K. Nadda, S. Chelliapan, A state-of-the-art review on the latest trends in hydrogen production, storage, and transportation techniques, Fuel 340 (2023) 127574, https://doi.org/10.1016/j.fuel.2023.127574.

[9] I.A. Hassan, H.S. Ramadan, M.A. Saleh, D. Hissel, Hydrogen storage technologies for stationary and mobile applications: review, analysis and perspectives, Renew. Sustain. Energy Rev. 149 (2021) 111311, https://doi.org/10.1016/j.rser.2021.111311.

[10] Y. Li, Q. Guo, Z. Ding, H. Jiang, H. Yang, W. Du, Y. Zheng, K. Huo, L.L. Shaw, MOFs-based materials for solid-state hydrogen storage: strategies and perspectives, Chem. Eng. J. 485 (2024) 149665, https://doi.org/10.1016/j.cej.2024.149665.

[11] M.D. Allendorf, V. Stavila, J.L. Snider, M. Witman, M.E. Bowden, K. Brooks, B. L. Tran, T. Autrey, Challenges to developing materials for the transport and storage of hydrogen, Nat. Chem. 14 (2022) 1214–1223, https://doi.org/10.1038/s41557-022-01056-2.

[12] D. Zhou, H. Sun, S. Guo, D. Zhao, J. Li, Y. Zhang, Hydrogen storage properties of Mg-based alloys modified with metal-organic frameworks and carbon-based porous materials: a review and summary, Int. J. Hydrogen Energy 57 (2024) 1373–1388, https://doi.org/10.1016/j.ijhydene.2024.01.127.

[13] L. Guo, J. Su, Z. Wang, J. Shi, X. Guan, W. Cao, Z. Ou, Hydrogen safety: an obstacle that must be overcome on the road towards future hydrogen economy, Int. J. Hydrogen Energy (2023), https://doi.org/10.1016/j.ijhydene.2023.08.248.

[14] H. Li, X. Cao, Y. Liu, Y. Shao, Z. Nan, L. Teng, W. Peng, J. Bian, Safety of hydrogen storage and transportation: an overview on mechanisms, techniques, and challenges, Energy Rep. 8 (2022) 6258–6269, https://doi.org/10.1016/j.egyr.2022.04.067.

[15] R. Moradi, K.M. Groth, Hydrogen storage and delivery: review of the state of the art technologies and risk and reliability analysis, Int. J. Hydrogen Energy 44 (2019) 12254–12269, https://doi.org/10.1016/j.ijhydene.2019.03.041.

[16] M. Hirscher, V.A. Yartys, M. Baricco, J. Bellosta von Colbe, D. Blanchard, R. C. Bowman, D.P. Broom, C.E. Buckley, F. Chang, P. Chen, Y.W. Cho, J.C. Crivello, F. Cuevas, W.I.F. David, P.E. de Jongh, R.V. Denys, M. Dornheim, M. Felderhoff, Y. Filinchuk, G.E. Froudakis, D.M. Grant, E.M.A. Gray, B.C. Hauback, T. He, T. D. Humphries, T.R. Jensen, S. Kim, Y. Kojima, M. Latroche, H.W. Li, M. V. Lototskyy, J.W. Makepeace, K.T. Møller, L. Naheed, P. Ngene, D. Noréus, M. M. Nygård, S.I.C.H.I. Orimo, M. Paskevicius, L. Pasquini, D.B. Ravnsbæk, M. Veronica Sofianos, T.J. Udovic, T. Vegge, G.S. Walker, C.J. Webb, C. Weidenthaler, C. Zlotea, Materials for hydrogen-based energy storage – past, recent progress and future outlook, J. Alloys Compd. 827 (2020) 153548, https://doi.org/10.1016/j.jallcom.2019.153548.

[17] F.D. Minuto, R. Balderas-Xicohténcatl, A. Policicchio, M. Hirscher, R.G. Agostino, Assessment methodology of promising porous materials for near ambient temperature hydrogen storage applications, Int. J. Hydrogen Energy 43 (2018) 14550–14556, https://doi.org/10.1016/j.ijhydene.2018.06.004.

[18] H. Kim, S.H. So, R. Muhammad, H. Oh, Comparing the practical hydrogen storage capacity of porous adsorbents: Activated carbon and metal-organic framework, Int. J. Hydrogen Energy (2023), https://doi.org/10.1016/j.ijhydene.2023.10.160.

[19] C. Altintas, S. Keskin, On the shoulders of high-throughput computational screening and machine learning: design and discovery of MOFs for H2 storage and purification, Materials Today Energy 38 (2023) 101426, https://doi.org/10.1016/j.mtener.2023.101426.

[20] A. Ahmed, S. Seth, J. Purewal, A.G. Wong-Foy, M. Veenstra, A.J. Matzger, D. J. Siegel, Exceptional hydrogen storage achieved by screening nearly half a million metal-organic frameworks, Nat. Commun. 10 (2019), https://doi.org/10.1038/s41467-019-09365-w.

[21] D.P. Broom, C.J. Webb, K.E. Hurst, P.A. Parilla, T. Gennett, C.M. Brown, R. Zacharia, E. Tylianakis, E. Klontzas, G.E. Froudakis, Th.A. Steriotis, P. N. Trikalitis, D.L. Anton, B. Hardy, D. Tamburello, C. Corgnale, B.A. van Hassel, D. Cossement, R. Chahine, M. Hirscher, Outlook and challenges for hydrogen storage in nanoporous materials, Applied Physics A 122 (2016) 151, https://doi.org/10.1007/s00339-016-9651-4.

[22] M. Yue, H. Lambert, E. Pahon, R. Roche, S. Jemei, D. Hissel, Hydrogen energy systems: a critical review of technologies, applications, trends and challenges, Renew. Sustain. Energy Rev. 146 (2021) 111180, https://doi.org/10.1016/j.rser.2021.111180.

[23] O. Schmidt, S. Melchior, A. Hawkes, I. Staffell, Projecting the future levelized cost of electricity storage technologies, Joule 3 (2019) 81–100, https://doi.org/10.1016/j.joule.2018.12.008.

[24] G. Zini, R. Marazzi, S. Pedrazzi, P. Tartarini, A solar hydrogen hybrid system with activated carbon storage, Int. J. Hydrogen Energy 35 (2010) 4909–4917, https://doi.org/10.1016/j.ijhydene.2009.09.014.

[25] G. Zini, P. Tartarini, Wind-hydrogen energy stand-alone system with carbon storage: modeling and simulation, Renew. Energy 35 (2010) 2461–2467, https://doi.org/10.1016/j.renene.2010.03.001.

[26] E. Rozzi, F.D. Minuto, A. Lanzini, Dynamic modeling and thermal management of a power-to-power system with hydrogen storage in microporous adsorbent materials, Journal of Energy Storage 41 (2021) 102953, https://doi.org/10.1016/j.est.2021.102953.

[27] A. Anastasopoulou, H. Furukawa, B.R. Barnett, H.Z.H. Jiang, J.R. Long, H. M. Breunig, Technoeconomic analysis of metal–organic frameworks for bulk hydrogen transportation, Energ. Environ. Sci. 14 (2021) 1083–1094, https://doi.org/10.1039/D0EE02448A.

[28] P. Peng, A. Anastasopoulou, K. Brooks, H. Furukawa, M.E. Bowden, J.R. Long, T. Autrey, H. Breunig, Cost and potential of metal–organic frameworks for hydrogen back-up power supply, nature, Energy 7 (2022) 448–458, https://doi.org/10.1038/s41560-022-01013-w.

[29] Net load profile for a 10 MWh hydrogen storage system, (n.d.). doi:https://doi.org/10.5281/zenodo.10259831.

[30] M.A. Richard, P. Bénard, R. Chahine, Gas adsorption process in activated carbon over a wide temperature range above the critical point. Part 2: conservation of mass and energy, Adsorption 15 (2009) 53–63, https://doi.org/10.1007/s10450-009-9150-4.

[31] A.I. Skoulidas, D.S. Sholl, Self-diffusion and transport diffusion of light gases in metal-organic framework materials assessed using molecular dynamics simulations, J. Phys. Chem. B 109 (2005) 15760–15768, https://doi.org/10.1021/jp051771y.

[32] R. Roszak, L. Firlej, S. Roszak, P. Pfeifer, B. Kuchta, Hydrogen storage by adsorption in porous materials: is it possible? Colloids Surf. A Physicochem. Eng. Asp. 496 (2016) 69–76, https://doi.org/10.1016/j.colsurfa.2015.10.046.

[33] L. Ding, A.O. Yazaydin, Hydrogen and methane storage in ultrahigh surface area metal-organic frameworks, Microporous Mesoporous Mater. 182 (2013) 185–190, https://doi.org/10.1016/j.micromeso.2013.08.048.

[34] J.J. Purewal, D. Liu, J. Yang, A. Sudik, D.J. Siegel, S. Maurer, U. Müller, Increased volumetric hydrogen uptake of MOF-5 by powder densification, Int. J. Hydrogen Energy 37 (2012) 2723–2727, https://doi.org/10.1016/j.ijhydene.2011.03.002.

[35] US DOE, Target explanation document: onboard hydrogen storage for light-duty fuel cell vehicles, U.S Drive (2017) 1–29.